

## **Physical Properties of Polymetallic Nodules and Deep Sea Sediments, as Determined with Different Analytical Techniques**

*Ivo Dreiseitl*

Interoceanmetal Joint Organization  
Szczecin, Poland

*Roman Bednarek*

West Pomeranian University of Technology  
Szczecin, Poland

### **ABSTRACT**

Description of physical properties of sediments and polymetallic nodules has been an essential part of geotechnical studies postulated in phase 2 of the “Plan of work for exploration for polymetallic nodules of InterOceanmetal (IOM)”. The relevant properties were determined in both shipboard and on-land laboratories. The shipboard analyses included sediment and nodule volumetric density ( $\rho$ ) and water content ( $w$ ), determined immediately after the samples had been retrieved. Other physical properties, such as dry unit weight ( $\rho_d$ ), porosity ( $n$ ), void ratio ( $e$ ), and specific density ( $\rho_s$ ) were calculated subsequently. Specific density ( $\rho_s$ ) was also determined in on-land laboratories using the pycnometric technique.

**KEY WORDS:** Polymetallic nodules; deep sea sediments; physical properties, pycnometric and other techniques

### **INTRODUCTION**

In 2009, sediment and polymetallic nodule samples were collected, using a box corer, from 50 stations visited during the InterOceanmetal Joint Organization (IOM) cruise to the IOM exploration area within the Clarion-Clipperton Fracture Zone (CCFZ) (approximate coordinates: 10.5°N, 120.2°W). Physical properties of sediments were determined on board (in the ship’s laboratory) on samples collected at 2-3 depth intervals in a box corer; physical properties of nodules were determined on 3-4 nodules picked up from each box core sample containing them. In land-based laboratories, corresponding analyses were conducted on 69 sediment and 30 nodule samples collected in a manner identical to that applied on board. Additional 30 nodule samples analyzed consisted nodule fragments collected with a dredge. Specific densities ( $\rho_s$ ) of the sediment and nodules resulting from on board computations and produced by pycnometric analyses were compared.

### **Deep Seabed (Pelagic) Sediments in IOM area: Brief Characteristics**

Kenneth (1982) suggested that pelagic sediments form via particle

sedimentation down the water column and include biogenic material, terrigenous clays and silts, pyroclastic materials blown through the air to the oceans, ice-rafted debris, and extraterrestrial material. In terms of grain size, such sediments are fine-grained and are mostly classified as clay or silty clay. The IOM research showed 70-85 and 20-25% of the samples to represent the 8 $\phi$ + (clay) and 4-8 $\phi$  (silty) fraction, respectively. Depending on their amorphous silica content, the clays (or silty clays) are divided into siliceous (10-30% SiO<sub>2am</sub>) and slightly siliceous (5-10 % SiO<sub>2am</sub>), as proposed by Kotlinski (2009). From the geotechnical standpoint, the deep seabed sediments within the IOM exploration area represent cohesive, highly plastic, inorganic soils. Microstructural analyses carried out by the IOM showed the particle arrangement to be disordered, which is a consequence of the intergranular contacts to be of the point-plane type (rarely plane-plane); as noted by Lu et al (2006), such particles, when subject to loading, may become displaced and broken.

### **Polymetallic Nodules in IOM area: Brief Characteristics**

Polymetallic nodules are natural, polymineral aggregates of ferromanganese hydroxides and clay minerals which, in terms of the chemical composition, consists of more than 50 elements (Kotlinski, 1998). Ferromanganese hydroxides precipitate on the nuclei formed by, e.g., fragments of old nodules and/or volcanic rocks, zeolites, fish teeth etc. In terms of their mode of formation, the nodules are classified into hydrogenous, diagenetic and hydrogenous-diagenetic, whereas morphologically they may be discoidal, ellipsoidal, spheroidal or tabular. From the standpoint of geotechnical research, nodules are coarse-grained, non-cohesive formations.

### **ANALYTICAL METHODS**

#### **Shipboard Analyses: Sediment**

Sediment samples were collected with cutting rings ( $\phi = 70$  mm;  $h = 50$  mm), as shown in Fig. 1, from a minimum of two levels of the original box corer content. This manner of sample collection is most appropriate due to the high cohesiveness of deep-sea sediments.



Fig. 1: Sediment sampling with cutting rings

The only physical properties determined in the ship's laboratory were the volumetric density and water content.

The volumetric density,  $\rho$  [ $\text{g}/\text{cm}^3$ ], is calculated with a well-known formula:

$$\rho = \frac{m}{V} \quad (1)$$

where:

$m$  = sediment sample weight  
 $V$  = sediment sample volume

The parameter is sometimes referred to as the moist unit weight,  $\rho_m$ .

The water content,  $w$  [%] is the amount of water contained in a material; it is expressed in terms of the mass of fresh water evaporated at  $105^\circ\text{C}$  per mass of **dried** material (an oven-dried sample):

$$w = \frac{m - m_1}{m_1 - m_2} \cdot 100 \quad (2)$$

where:

$m$  = weight of wet material with weight of weighing bottle [g]  
 $m_1$  = weight of dried material with weight of weighing bottle [g]  
 $m_2$  = weight of weighing bottle [g]

During evaporation, the pore water-contained salts precipitate in the sediment pores, so the result has to be corrected for pore water mineralization. Then the true water content,  $w'$ , is given by:

$$w' = \frac{w(1 + M)}{1 - Mw \cdot 0.01} \quad (3)$$

where:

$w$  = water content of material without correction for pore water mineralization [%]  
 $M$  = pore water mineralization  $M = 0.035$

Based on the results of calculations, other physical properties, such as dry unit weight, porosity, void ratio, and specific unit weight are computed. The dry unit weight  $\rho_d$  [ $\text{g}/\text{cm}^3$ ] is based on the solids weight to the total volume ratio, as given by:

$$\rho_d = \frac{\rho}{1 + w' \cdot 0.01} \quad (4)$$

where:

$\rho$  = volumetric density obtained previously  
 $w'$  = water content corrected for pore water mineralization.

In the deep-sea sediments, seawater fills the spaces between solid particles. The amount of the spaces can be expressed by each of the following two parameters: porosity and void ratio (e.g., Zaruba and Mencl, 1976). Porosity,  $n$ , represents the proportion of the total volume of the material mass occupied by spaces and is calculated as:

$$n = w' \frac{\rho_d}{\rho_{pw}} \quad (5)$$

where:

$w'$  = water content corrected for pore water mineralization

$\rho_d$  = dry unit weight

$\rho_{pw}$  = unit weight (density) of pore water with  $M = 0.035$  at  $t = 20^\circ\text{C}$  ( $\rho_{pw} = 1.025 \text{ g}/\text{cm}^3$ )

The void ratio,  $e$ , expresses the relationship between the volume of space and the volume of solids within the volume of the total mass:

$$e = \frac{n}{100 - n} \quad (6)$$

where  $n$  = porosity [%]

The dry unit weight and void ratio are used to calculate the specific (solid particles) density,  $\rho_s$ , as in:

$$\rho_s = \rho_d(1 + e) \quad (7)$$

The specific density can be obtained also using the pycnometric technique in an on-land laboratory, as described further on in the paper.

### Atterberg Limits

Johnson and De Graaf (1988) noted that the amount of water in the soil controls the deformation behavior in that soil. This behavior is called soil consistency. Consistency of a particular soil is defined by the water content present when it changes its response to stress. The changes are called the Atterberg limits and expressed in %. The plastic limit,  $PL$ , is the water content when soil begins to exhibit plastic behavior. The liquid limit,  $LL$ , is the water content when soil changes from plastic to liquid state (Figs. 2, 3).

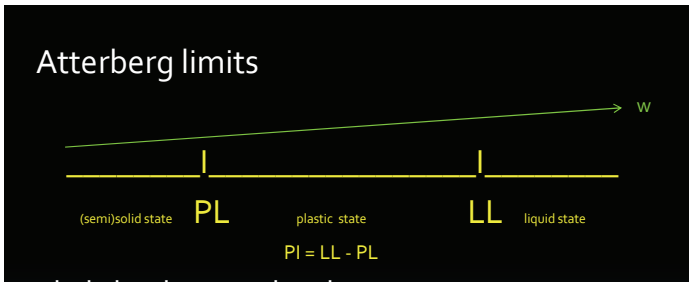


Fig. 2: The Atterberg limits ( $PL$ ,  $LL$ ) and increasing water content  $w$

$LL$  is determined with the cone penetrometer test and involves measuring the depth of penetration into the soil of a standardized cone of a specific mass. In the IOM research, a 76 g  $30^\circ$  angle stainless steel cone was released for 5 seconds so that it penetrated the soil.  $LL$  was defined as the water content of the soil which allowed the cone to penetrate 10 mm during 5 seconds.  $PL$  is calculated with the Spikov formula, as proposed by Neizvestnov and Kondratenko (2004):

$$PL = LL - 0.55 (LL - 0.11) \quad (8)$$

The plasticity index,  $PI$  [%], is the difference between the liquid limit and the plastic limit:

$$PI = LL - PL \quad (9)$$

In the range of water contents measured, the sediments exhibited plastic properties (Figs. 2, 3). The sediments in the IOM area showed high  $PI$ s, confirming their clayey nature.

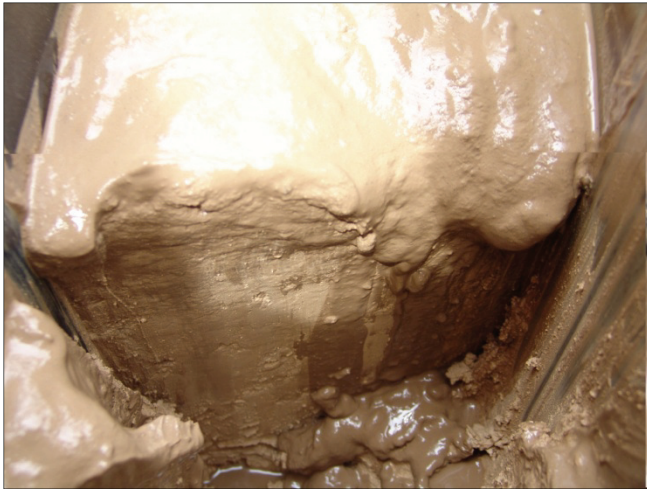


Fig. 3: Liquid (at the surface) and plastic (below) consistencies of deep-sea sediments

## Nodules

Most of the physical properties of nodules (volumetric density, dry unit weight, specific weight, porosity, void ratio) were determined in a manner identical to that applied to the sediment. The only exception was the water content; here, two parameters were identified: one determined as in formula (2) and the other, called the “natural” water content,  $w_n'$ , is expressed as the mass of water evaporated at  $105^\circ\text{C}$  relative to the mass of a wet nodule sample:

$$w_n' = \frac{w_n(1 + M)}{1 - Mw_n \cdot 0.01} \quad (10)$$

where:

$w_n'$  = “natural” water content (without correcting for mineralization) [%]

$M = 0.035$  nodule water mineralization correction

Similarly to the procedure applied to the sediment, the nodule specific weight was also determined pycnometrically in the on-land laboratory.

## Analyses in On-land laboratory

As mentioned above, the on-land laboratory allows to determine one parameter only, i.e., the specific weight of both the sediment and nodules. The determinations were conducted on dried and crumbled sediment and nodules. The density of solid particles is calculated by dividing their mass,  $M_d$ , by volume,  $V_d$ .

$$\rho_s = \frac{M_d}{V_d} \quad (11)$$

where:

$M_d$  = mass of solid particles

$V_d$  = volume of solid particles.

Initially, solid particles are weighed to obtain the mass of dry soil and the volume of solid particles is calculated. The pycnometric technique can be used for determining the specific density values of solid particles of both fine- and coarse-grained soils. The technique involves determination of the volume of a known soil mass using displacement. The density of solid particles is calculated from the mass and volume of the soil. Pycnometric density determination is very precise. Distilled water of known density is used as the displacement liquid. To apply the pycnometric technique, weight of the dry pycnometer, weight of the pycnometer together with an inserted object, weight of the pycnometer together with the inserted object and distilled water, and weight of the pycnometer filled with water only have to be known. The following formula is applied then:

$$V_d = \frac{m_{wt} + (m_{gt} - m_t) - m_{wgt}}{\rho_w} \quad (12)$$

where:

$m_{wt}$  = weight of pycnometer with water

$m_t$  = weight of dry pycnometer

$m_{wgt}$  = weight of pycnometer together with soil and water

$m_{gt}$  = weight of pycnometer with dry soil

$\rho_w$  = distilled water density.

The results will be precise only if the pycnometer is used at the same temperature throughout the procedure. The temperature is very important as the distilled water density is temperature-dependent.

Soil particles sometimes contain enclosed voids which are included in the volume  $V_d$ . For this reason, the apparent density of solid particles is determined. The standard procedure of density determination involves the use of a density bottle (pycnometer) to determine the volume of the soil specimen by water displacement. A sample of about 30 g dry soil is placed in the density bottle, distilled water is added, and the content is

de-aired., The value of  $\rho_s$  is calculated from the measured masses and the known density of water. A liquid different than distilled water (e.g., trichloroethylene, kerosene, toluene) may be necessary for soils containing materials that react with water.

## RESULTS

Since 2001, when the IOM concluded the Contract for Exploration with the International Seabed Authority (ISA), the IOM has amassed a substantial amount of data on physical properties of sediments and nodules, determined using a uniform methodology. The existing database has been extended by inclusion of validated geotechnical data from the earlier stage of prospection of the exploration area.

### Sediment

According to the classification of sediment types encountered in the IOM exploration area (Kotliński, 2009), the following types can be discerned:

1. Siliceous silty clay
2. Slightly siliceous silty clay
3. Red pelagic clays with zeolites
4. Radiolarian ooze
5. Diatom ooze
6. Zeolitic crusts.

Table 1 reports the measured (m) and computed (c) physical properties (the maximum and minimum values) of the sediment types listed above. The data, from a total of 4512 analyses (see denominators in Table 1), were obtained in shipboard laboratory during cruises to the exploration area.

Table 1. Physical properties of sediments in the IOM exploration area

Type	$\rho_s$ , g/cm <sup>3</sup>	$w'$ , %	$\rho_{ds}$ , g/cm <sup>3</sup>	$n_s$ , %	$e$	$\rho_s$ , g/cm <sup>3</sup>
m/c	m	m	c	c	c	c
1	<u>1.17-1.24</u> 208	<u>254-414</u> 218	<u>0.23-0.36</u> 208	<u>86-92</u> 208	<u>6.05-11.23</u> 208	<u>2.48-3.02</u> 208
2	<u>1.18-1.28</u> 389	<u>210-404</u> 406	<u>0.27-0.40</u> 389	<u>84-91</u> 389	<u>5.09-10.02</u> 389	<u>2.40-3.07</u> 389
3	<u>1.20-1.33</u> 79	<u>170-302</u> 82	<u>0.31-0.49</u> 79	<u>82-89</u> 79	<u>4.44-7.95</u> 79	<u>2.42-2.86</u> 79
4	<u>1.12-1.25</u> 22	<u>255-591</u> 28	<u>0.16-0.35</u> 22	<u>87-95</u> 22	<u>5.95-17.3</u> 22	<u>2.05-3.00</u> 22
5	<u>1.16-1.20</u> 35	<u>319-437</u> 39	<u>0.22-0.29</u> 35	<u>88-92</u> 35	<u>7.66-11.86</u> 35	<u>2.35-2.95</u> 35
6	<u>1.32-1.56</u> 14	<u>85-185</u> 12	<u>0.46-0.84</u> 12	<u>70-84</u> 12	<u>2.35-5.11</u> 12	<u>2.46-2.96</u> 12
$\Sigma$	747	785	745	745	745	745

In the 2009 cruise, a total of 123 samples of different sediment types were processed on board to yield 738 new geotechnical data entries (123 samples x 6 properties).

Table 2 shows Atterberg limits data for various sediment types, except for crusts which are impossible to be penetrated by the cone.

Table 2. Atterberg limits of sediments

Type	$LL$ , %	$PL$ , %	$PI$ , %
m/c	m	c	c
1	<u>116-241</u> 7	<u>58-121</u> 7	<u>58-120</u> 7
2	<u>110-186</u> 18	<u>56-96</u> 18	<u>55-90</u> 18
3	<u>80-277</u> 17	<u>38-140</u> 17	<u>42-137</u> 17
4	<u>103-357</u> 10	<u>51-190</u> 10	<u>52-167</u> 10
5	<u>142</u> 1	<u>70</u> 1	<u>72</u> 1

Fig. 4 shows the relationship between the volumetric density and the amorphous silica content in the sediment. The data points in the graph denote a total of 90 samples. The trend line has never been more clear-cut. It conforms to the assumption that the lower the  $SiO_{2am}$  content in a sediment sample, the denser the sediment.

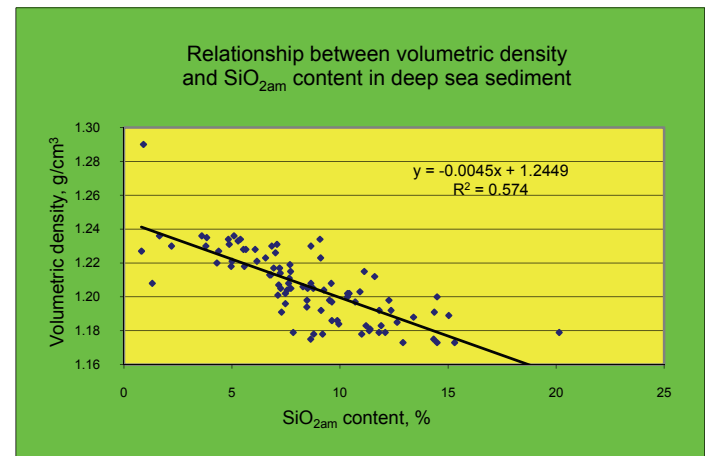


Fig. 4: Relationship between volumetric density and amorphous silica content in sediment

As noted in the Analytical Methods section above, the specific density can be determined also in an on-land laboratory using the pycnometric technique. To compare the computed and (pycnometrically) measured specific densities, a total of 69 samples were processed in a dedicated geotechnical laboratory<sup>1</sup> in 2010. Table 3 reports the results of pycnometric measurements and provides a comparison between the computed and measured specific densities.

Table 3. Comparison of computed and measured specific densities

Nr	Station	Interval, cm	Sediment type	Remarks	$\rho_s$ , g/cm <sup>3</sup>	
					calcul	pycno
1	2262	10-15	SIL		2.75	2.64
2		30-35	SLSIL		2.75	2.69
3	2263	10-15	SLSIL→ZC		2.91	2.70
4	2264	0-5	SLSIL	GAL <sup>2</sup>	nd	2.70
5		10-15	SLSIL		2.85	2.67

<sup>1</sup> Geotechnical laboratory of the West Pomeranian University of Technology, Szczecin, Poland

<sup>2</sup> Geochemically active layer

6	2265	10-15	SLSIL		2.81	2.64
7	2266	10-15	SLSIL		2.82	2.69
8	2267	10-15	SLSIL		2.96	2.65
9	2268	10-15	SLSIL		2.81	2.66
10	2269	20-25	ZC		2.88	2.70
11	2270	10-15	SLSIL		2.78	2.68
12	2271	15-20	SIL		2.68	2.66
13	2272	12-17	SIL		2.52	2.65
14	2273	10-15	SLSIL		2.77	2.70
15	2274	10-15	SLSIL→ZC		2.82	2.75
16	2275	10-15	SIL		2.92	2.64
17	2276	10-15	SLSIL		2.77	2.73
18	2277	10-15	SLSIL		2.82	2.65
19	2278	10-15	SLSIL		3.01	2.68
20		25-30	SLSIL		3.04	2.68
21	2279-1	10-15	SLSIL		2.78	2.61
22	2280	10-15	SIL		2.76	2.56
23	2281	10-15	SLSIL→SIL		2.77	2.65
24	2282	12-17	SIL		2.80	2.57
25	2283	10-15	SLSIL		2.88	2.66
26	2284	10-15	SIL		2.65	2.63
27	2285	12-17	SLSIL		2.83	2.63
28	2286	12-17	ZC		2.80	2.64
29	2287	15-20	ZC		2.81	2.71
30	2288	3-6	SLSIL	GAL	2.90	2.56
31		10-15	SIL		2.70	2.60
32	2289	3-6	SLSIL	GAL	2.91	2.50
33		10-15	SIL		2.85	2.61
34	2290	2-5	SLSIL	GAL	2.97	2.65
35		10-15	SIL		2.67	2.65
36	2291	10-15	SIL		2.91	2.63
37		25-30	SLSIL		3.07	2.60
38	2292	10-15	SIL		2.74	2.57
39	2293	2-5	SIL	GAL	2.70	2.65
40		10-15	SIL		2.66	2.62
41	2294	3-6	SIL	GAL	2.63	2.62
42		10-15	SLSIL		2.91	2.66
45	2295	6-9	SIL		2.69	2.76
46	2296	9-11	ZCr		nd	2.53
47		13-18	ZC		2.70	2.76
48	2297	2-5	SIL	GAL	2.66	2.52
49		10-15	SLSIL→SIL		2.77	2.54
50	2298	4-7	SLSIL		2.65	2.50
51		10-15	SLSIL		2.78	2.53
52	2299	2-5	SLSIL	GAL	2.75	2.41
53		10-15	SIL		2.65	2.49
54	2300	10-15	SLSIL→SIL		2.80	2.49
55	3001	10-15	SLSIL→SIL		2.75	2.48
56	3002	10-15	SIL		3.02	2.49
57	3003	10-15	SIL		2.59	2.51
58	3004	10-15	SIL		2.72	2.43
59	3005	2-5	SIL		2.87	2.48
60		12-17	ETM		2.67	2.45
61	3006	10-15	SLSIL→SIL		2.79	2.49
62	3007	10-15	SLSIL→SIL		2.85	2.49
63	3008	10-15	SIL		2.42	2.51
64		25-30	SIL		2.80	2.50
65	3011	15-20	ZC		2.83	2.64
66	3015	10-15	SLSIL		2.79	2.48
67	3016	2-5	SLSIL→SIL	GAL	2.60	2.55
68		10-15	SLSIL→SIL		2.89	2.45
69	3017	13-18	SLSIL		2.96	2.61

avg	2.79	2.60
max	3.07	2.76
min	2.42	2.41
med	2.79	2.63
stdev	0.1228	0.0882

where:

SIL, siliceous silty clay

SLSIL, slightly siliceous silty clay

ZC, red pelagic clays with zeolites

ETM, diatom ooze

ZCr, zeolitic crusts

SLSIL→ZC, SLSIL→SIL, transitional forms of sediments

The descriptive statistical metrics reported in Table 3 generally show the densities determined pycnometrically to be lower than the computed values. The difference between the maximums ( $0.31 \text{ g/cm}^3$ ) and median values ( $0.16 \text{ g/cm}^3$ ) are fairly substantial, whereas the minimum values can be considered as comparable. The lower standard deviations of the pycnometric data confirms the better accuracy of determinations made in the on-land laboratory.

The case in point is illustrated by slightly siliceous clay, the most frequent sediment type in the IOM exploration area (Fig. 5).

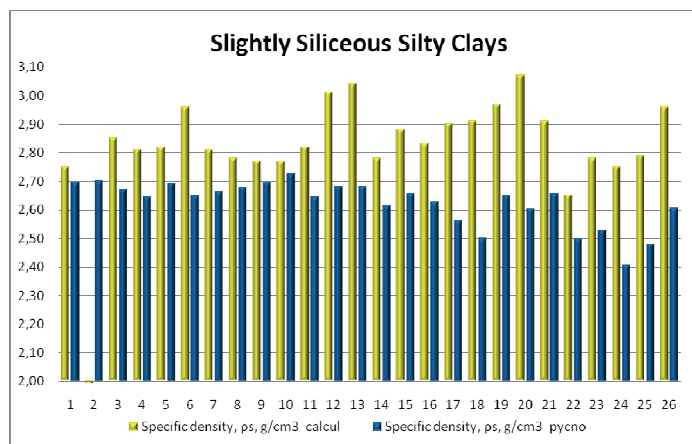


Fig. 5: Specific densities of slightly siliceous clay as determined by computation and with pycnometric technique applied to 26 sediment samples.

A total of 52 specific density data points, measured in 26 samples of slightly siliceous silty clay (from the 2009 cruise only) are presented. It is evident that, compared to the computed data, the pycnometric results span a narrower range, particularly in the first 21 samples. The statistical metrics are as follows:

Pycno.:

avg 2.62  
max 2.73  
min 2.41  
med 2.65  
stdev 0.0802

Calcul.:

avg 2.85  
max 3.07  
min 2.65  
med 2.82  
stdev 0.1031.

## Nodules

The physical properties of nodules were determined in the manner identical to that applied to the sediment. The following genetic nodule types (genotypes) were distinguished (e.g. Kotlinski, 1999):

D, diagenetic

D<sub>1</sub>, diagenetic (Cu > Ni)

HD, hydrogenous-diagenetic

H, hydrogenous.



Table 4 summarizes the physical properties of different nodule genotypes. Each property was determined from 447 measurements or computations. Nodules occurring in the IOM exploration area are dominated by the diagenetic (D, D<sub>1</sub>) genotype. The last row in Table 4 shows arithmetic mean  $\bar{\rho}$  of the principal physical properties of those two genotypes.

Table 4. Basic physical properties of various nodule genotypes

Type	$\rho_s$ , g/cm <sup>3</sup>	$w'$ , %	$w'_{n_s}$ , %	$n_s$ , %	$e$	$\rho_{s_s}$ , g/cm <sup>3</sup>
m/c	m	m	m	c	c	c
D	1.75-2.08 256	39-66 256	28-34 256	55-69 256	1.21-2.18 256	3.08-3.60 256
D <sub>1</sub>	1.77-2.03 143	42-64 143	30-39 143	58-68 143	1.39-2.15 143	3.22-3.59 143
HD	1.83-2.04 33	39-56 33	28-36 33	55-65 33	1.21-1.87 33	3.14-3.54 33
H	1.92-2.01 15	38-49 15	28-33 15	54-63 15	1.18-1.67 15	3.16-3.52 15
$\Sigma$	447	447	447	447	447	447
$\bar{\rho}$ D+D <sub>1</sub>	1.95	48	32	61	1.57	3.41

The histogram of frequency distribution of the specific nodule densities (Fig. 6) confirms  $\rho_s = 3.30-3.39$  g/cm<sup>3</sup> to be the most frequent range in both the 1988 and 2009 cruise.

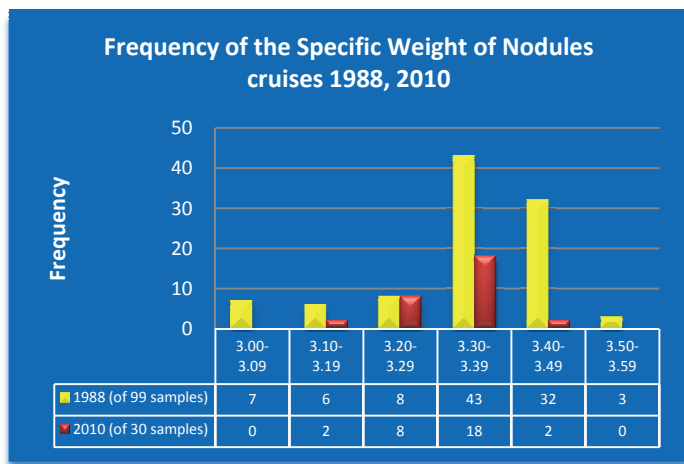


Fig. 6: Frequency of specific nodule density by selected intervals

Pycnometric technique was applied in the on-land laboratory to 30 genotype D and D<sub>1</sub> nodule fragments collected with a dredge during the 2009 cruise. As shown by Table 5, the data are well correlated ( $\sigma = 0.0732$ ), the correlation being stronger than that for corresponding data obtained in the 1988 cruise ( $\sigma = 0.1159$ ).

Table 5. Basic statistical metrics of specific nodule density

$\rho_s$ , g/cm <sup>3</sup>	Cruise 1988 pycnometric	Cruise 2009	
		computed	pycnometric
$\bar{\rho}$	3.34	3.33	3.31
max	3.58	3.68	3.45
min	3.04	3.14	3.12
$\sigma$ , no unit	0.1159	0.1414	0.0732

## CONCLUSIONS

- Pycnometric determination of physical properties (primarily the specific density) of sediment and nodules in an on-land laboratory is very important for geotechnical research as a way to supply the true and most accurate data on the property being determined.
- Generally, the specific densities of sediment, as determined pycnometrically, were lower than those produced by computation.
- The pycnometric data on sediment and nodules are better correlated than the computed data.
- The void ratios of deep-sea clays containing amorphous silica show the spaces between solid particles to be 10 times higher than the volume of the solid particles. In D D<sub>1</sub> nodules, the space to particle volume ratio is about 2 (the space between solid particles twice as large as the solid particle volume).
- The Atterberg numbers obtained confirm highly plastic and liquid consistencies of the deep-sea sediments analyzed.
- In the 1988 and 2009 cruises, the most frequent nodule density range, as determined pycnometrically, was  $\rho_s = 3.30-3.39$  g/cm<sup>3</sup>.
- Based on the 447 determinations of the nodule natural water content, it can be claimed that water accounts for about 1/3 of the nodule volume.

## ACKNOWLEDGMENT

The research presented was carried out as a part of exploration activities at stage 2 of the contract with ISA and was supported by the IOM certifying states. The authors are grateful to the West Pomeranian University of Technology in Szczecin, Poland, for making the geotechnical laboratory available for the analyses.

## REFERENCES

- Depowski, S, Kotlinski, R et al (1998). *Surowce Mineralne Morz i Oceanow*, Scholar, pp 101-113, 127, 163.
- Johnson, RB, and De Graaf, JV (1988). *Principles of Engineering Geology*, John Wiley & Sons, pp 77-87.
- Kennett, JP (1982). *Marine Geology*, Prentice Hall, pp 397-401.
- Kotlinski, R (1999). *Metallogenesis of the World's Ocean against the Background of Oceanic Crust Evolution*, Special Papers 4, Polish Geological Institute, pp 24-39.
- Kotlinski, R, and Stoyanova V (2009). Relationship between Nodule Coverage, Morphology and Distribution in the Eastern CCZ, in: Morgan ChL (ed) *Prospectors Guide for the Clarion-Clipperton Zone Polymetallic Nodule Deposits*, ISA, pp 1-13.
- Lu, B, Li, G et al (2006). Physical Properties of Sediments on the Northern Continental Shelf of the South China Sea. *Marine Georesources & Geotechnology*, Vol 24 No 1, pp 47-60.
- Neizvestnov, JaV, Kondratenko, AV et al (2004). *Engineering Geology of the Clarion-Clipperton Ore Province in the Pacific Ocean*, Nauka, pp 60-66.
- Zaruba, Q, and Mencl, V (1976). *Engineering Geology*, Academia Prague, pp 29-35.